The Journal of Antibiotics (2018) 71:808–817
https://doi.org/10.1038/s41429-018-0066-7

JARA Japan Antibiotics Research Association
The Society for Actinomycetes Japan

ARTICLE

Bafilomycin C1 induces G0/G1 cell-cycle arrest and mitochondrial-mediated apoptosis in human hepatocellular cancer SMMC7721 cells

Xiaoxiao Gao[1] · Li Han[1] · Nan Ding[1] · Yu Mu[1] · Peipei Guan[1] · Caijuan Hu[1] · Xueshi Huang[1]

Received: 1 February 2018 / Revised: 8 April 2018 / Accepted: 15 April 2018 / Published online: 11 May 2018

Abstract

Bafilomycin C1, which was isolated from *Streptomyces albolongus* in our previous work, exhibited strong cytotoxicity against several cancer cell lines. This study aimed to evaluate its antitumor effect on human hepatocellular cancer SMMC7721 cells and the underlying mechanism in vitro and in vivo. MTT assay revealed that bafilomycin C1 retarded SMMC7721 cell growth and proliferation. Western blot and real-time qPCR analysis revealed that bafilomycin C1 caused partial G0/G1 phase cell-cycle arrest, downregulated the expression of cyclin D3, cyclin E1, CDK2, CDK4, and CDK6 and upregulated the expression of p21. Moreover, bafilomycin C1 caused mitochondrial membrane dysfunction through oxidative stress. Furthermore, bafilomycin C1 decreased the expression of Bcl-2; increased the expression of Bax, p53, and P-p53; and increased cleavage of caspase-9 and caspase-3, thereby inducing the intrinsic caspase-dependent apoptotic pathway. In vivo experiments in mice suggested that bafilomycin C1 suppressed tumor growth with few side effects. Cell-cycle arrest and induced apoptosis in tumor tissues in a mouse model treated with bafilomycin C1 were demonstrated by histological analyses, western blot and TUNEL. These findings indicate that bafilomycin C1 may be a promising candidate for hepatic cellular cancer therapy.

Introduction

Hepatocellular carcinoma (HCC), which is closely linked to infection and chronic liver disease, is one of the most common malignancies with a very high mortality [1]. To date, there is no effective chemotherapy available to the large numbers of HCC patients. Surgical therapy is contraindicated for large majority of patients because of their poor liver function [2, 3]. In addition, HCC is highly resistant to multiple chemotherapeutic agents [4].

In the process of discovering new antibacterial and antitumor active agents from microbial sources, nine cytotoxic bafilomycins were isolated from the fermentation broth of *Streptomyces albolongus* by our research group [5]. Among them, bafilomycin C1 presented the strongest cytotoxic activity, especially against SMMC7721 HCC cells [5]. Bafilomycin C1 was first isolated from *Streptomyces griseus* and had shown multifunctional bioactivities, including antifungal activity, cellular cytotoxicity, and inhibition of vacuolar H^+ ATPase [6–10]. Recently, the molecular mechanisms responsible for the antifungal effect of bafilomycin C1 were elucidated by our research group [10]. However, the mechanism for the antitumor effect of bafilomycin C1 has still not been reported. To explore the potential of bafilomycin C1 for treatment of HCC, the effect of bafilomycin C1 on proliferation, cell-cycle arrest, and inducing apoptosis of HCC SMMC7721 and HepG2 cells in vitro and xenograft growth inhibition in vivo as well as the underlying mechanism were investigated in the present study.

Materials and methods

General experimental procedures

Bafilomycin C1 was isolated from a fermentation broth of *S. albolongus* by previously described method [5]. The fermentation broth was treated with the polymeric resin

✉ Li Han
hanli@mail.neu.edu.cn

✉ Xueshi Huang
huangxs@mail.neu.edu.cn

[1] Institute of Microbial Pharmaceuticals, College of Life and Health Sciences, Northeastern University, 110819 Shenyang, P. R. China

Amberlite XAD-16 to capture bound compounds. The crude extract was then isolated by sequential chromatography over Sephadex LH-20 and silica gel to yield bafilomycin C1 with a purity of 98.0% as determined by high-pressure liquid chromatography. Bafilomycin C1 was dissolved in dimethyl sulfoxide (DMSO) to prepare a 100 μM stock solution and stored at −20 °C. Working solutions of bafilomycin C1 were prepared by diluting the stock solution with DMSO prior to use.

Cell culture

Human HCC cell lines SMMC7721 and HepG2 (obtained from Chinese Academy of Sciences, Shanghai, China) were cultured in RPIM-1640 and Dulbecco's modified Eagle's medium culture medium, respectively, with 10% fetal bovine serum, 1% L-glutamine, 100 units/mL penicillin, and 100 μg/mL streptomycin at 37 °C in a humidified 5% CO_2 atmosphere incubator (Thermo Fisher Scientific, Waltham, USA).

Cell viability assay

The cell viability was quantified by the 3-[4,5-dimethylthiazol-2-yl]-2,5 diphenyl tetrazolium bromide (MTT) assay [11]. SMMC7721 and HepG2 cells were seeded in 96-well plates at a density of 7×10^3 cells/well and exposed to bafilomycin C1 at different concentrations (0.33, 1.1, and 3.3 μM for SMMC7721; 1.1, 3.3, and 10.0 μM for HepG2) for 6 days, respectively. After incubation at 37 °C for various periods of time (0, 1, 2, 3, 4, 5, and 6 days, respectively), 20 μL MTT (5 mg/mL in 1× phosphate-buffered saline (PBS)) was added into each well and incubated another 4 h. After that, the liquid in the well was removed and 150 μL DMSO was added into each well. A microplate reader (BioTek Synergy H1, BioTek Instruments, Inc., Vermont, USA) were used at 570 nm to measure the absorbance of each well. Inhibition rate (%) = $[(A_{570}(\text{control}) - A_{570}(\text{bafilomcycin C1})]/A_{570}(\text{control}) \times 100\%$. The results are represented as mean ± SD from three independent experiments.

Measurement of cell-cycle arrest

SMMC7721 and HepG2 cells were seeded in a 6-well plate at a density of 5×10^5 cells/well, respectively, and treated with vehicle or bafilomycin C1 (3.3 μM for SMMC7721; 10.0 μM for HepG2) for 24 h. Treated cells were trypsinized, centrifuged, and washed with cold PBS, fixed with 75% ethanol, and then left overnight at −20 °C. Following adequate washing with PBS, the fixed cells were incubated with propidium iodide (PI) working solution for 30 min in the dark at room temperature [12]. Samples were immediately run on a flow cytometer (BD, LSRFortesssa, USA) with a total of 20,000 cells collected and analyzed with the PI-based cell-cycle phase. The results are represented as mean ± SD from three independent experiments.

Hoechst 33258 staining

Cells stained with Hoechst 33258 (Beyotime Biotechnology Co., Shanghai, China) were used to evaluate the morphological changes [13]. Briefly, 10^5 cells/well were seeded in 6-well plates and treated with vehicle or bafilomycin C1 (3.3 μM) for 24 h. Then treated cells were fixed with paraformaldehyde for 5 min, washed twice with PBS, and stained with 500 μL Hoechst 33258 for 5 min in the dark at room temperature. Morphological changes were evaluated by a fluorescence microscope (Leica, DMi8, Gremany)

Measurement of apoptosis

SMMC7721 and HepG2 cells were seeded in a 6-well plate at a density of 5×10^5 cells/well, respectively, and treated with vehicle or bafilomycin C1 (3.3 μM for SMMC7721; 10.0 μM for HepG2) for 24 h. Then, cells were trypsinized, centrifuged, and washed with cold PBS and re-suspended in 490 μL of the provided binding buffer. A total of 5 μL fluorescein isothiocyanate (FITC)-labeled Annexin V (BD, Franklin Lakes, NJ, USA) and 5 μL PI were added to the samples and mixed gently. Samples were immediately run on a flow cytometer, with a total of 20,000 cells collected and analyzed with the Annexin V-FITC/PI apoptosis method after 15 min incubation in the dark at room temperature [14]. The results are represented as mean ± SD from three independent experiments.

Measurement of intracellular reactive oxygen species (ROS) generation

Intracellular ROS level was quantified by 2',7'-dichlorodihydrofluorescein diacetate (DCFH-DA) probe (Sigma-Aldrich, Darmstadt, Germany) [15]. SMMC7721 cells were seeded in a 6-well plate at a density of 5×10^5 cells/well and pre-treated with *N*-acetylcysteine (NAC; 5 mM) or vehicle for 1 h. Then vehicle or different concentrations of bafilomycin C1 (0.33, 1.1, and 3.3 μM) were added into the treated cells for 24 h. After that, cells were incubated with DCFH-DA (10 μM) dissolved in serum-free medium for 20 min at 37 °C in the dark. Cells were washed twice with PBS and lysed with 700 μL RIPA. A microplate reader with fluorescence intensity of 480 nm excitation wavelength and 530 nm emission wavelength were used to detect intracellular ROS production. The results are represented as mean ± SD from three independent experiments.

Measurement of mitochondrial membrane potential (MMP)

MMP was measured using JC-1 probe (Beyotime Biotechnology Co., Shanghai, China) [16]. SMMC7721 cells were seeded in a 6-well plate at a density of 5×10^5 cells/well and treated with vehicle or different concentrations of bafilomycin C1 (0.33, 1.1, and 3.3 μM) for 24 h. Then cells were incubated with a JC-1 staining solution (5 μg/mL) at 37 °C for 20 min in the dark, washed twice with PBS, and resuspended in the buffer. The "monomer" at low membrane potential was detected by a green fluorescence (514 nm excitation wavelength, 529 nm emission wavelength); and the "J-aggregates" at higher potential existed as a red fluorescence (585 nm excitation wavelength, 590 nm emission wavelength). The green/red fluorescence intensity ratio indicated the loss of MMP. The results are represented as mean ± SD from three independent experiments.

Synthesis of ATP assay

The cellular ATP level was determined by an ATP Bioluminescence Assay Kit (Beyotime Biotechnology Co., Shanghai, China) [17]. SMMC7721 cells were seeded in a 6-well plate at a density of 5×10^5 cells/well and treated with vehicle or different concentrations of bafilomycin C1 (0.33, 1.1, and 3.3 μM) for 24 h. After that, cells were lysed and centrifuged, and supernatants were obtained. Then 100 μL working solution as well as 20 μL supernatant were added to 96-well plate and mixed gently according to the manufacturer's instructions. Luminescence was immediately measured on a microplate reader. Measurements from all samples were normalized to the protein concentration. The results are represented as mean ± SD from three independent experiments.

RNA extraction and real-time PCR

The effect of bafilomycin C1 on the gene expression was examined in SMMC7721 cells using SYBR Green real-time quantitative PCR (qPCR) (Applied Biosystems, StepOne Real-Time PCR System, USA) [18]. SMMC7721 cells were seeded in a 6-well plate at a density of 5×10^5 cells/well and treated with vehicle or bafilomycin C1 (3.3 μM) for 24 h. The total RNA from treated cells was extracted using TRIzol Reagent (Ambion, Foster City, CA, USA) according to the manufacturer's instructions. The cDNA was synthesized from the extracted total RNA using the GoScript™ reverse transcription system (Promega, Madison, WI, USA). The sense and anti-sense primers for the amplification of each fragment are as follows: *Cyclin D3* 5'-AGCGCCTTTCCCAACTCTA-3' and 5'-CCAGGGTTACCACCACTTGT-3'; *Cyclin E1* 5'-GCTCGGGCTTTGTCCAG-3' and 5'-CTTCCTGGACACGCTGGT-3'; *CDK2* 5'-CCTTGTTTGTCCCTTCTAC-3' and 5'-CAAATCCACCCACTATGA-3'; *CDK4* 5'-CCTCTTTGGCAGCTGGTCAC-3' and 5'-ACCGACACCAATTTCAGCCA-3'; *CDK6* 5'-CTGAATGCTCTTGCTCCTTT-3' and 5'-AAAGTTTTGGTGGTCCTTGA-3'; *p21* 5'-AGGCACCGAGGCACTCAGAG-3' and 5'-TGACAGGTCCACATGGTCTTCC-3'; *Bax* 5'-CTGAGCAGATCATGAAGACA-3' and 5'-AGTTTGCTGGCAAAGTAGAA-3'; *Bcl-2* 5'-CTTTGAGTTCGGTGGGGTCA-3' and 5'-GGGCCGTACAGTTCCACAAA-3'; *p53* 5'-TCTACAAGCAGTCACAGCAC-3' and 5'-CTGGAGTCTTCCAGTGTGAT-3'; and glyceraldehyde 3-phosphate dehydrogenase (*GAPDH*) 5'-GGCAAGTTCAATGGCACAGT-3' and 5'-TGGTGAAGACGCCAGTAGACTC-3'. Real-time qPCR was performed at 95 °C for 10 s, 60 °C for 20 s, and 72 °C for 20 s for a total of 35 cycles and *GAPDH* was used as an internal control. The $2^{-\Delta\Delta CT}$ method was used to analyze relative changes in gene expression for statistical analysis [19].

Western blotting analysis

For in vitro experiments, SMMC7721 cells were seeded in a 6-well plate at a density of 8×10^5 cells/well and treated with vehicle or different concentrations of bafilomycin C1 (0.33, 1.1, and 3.3 μM) for 24 h, then washed with cold PBS, and lysed with RIPA lysis buffer (Beyotime Biotechnology Co., Shanghai, China) containing 2% protease inhibitor cocktail (Promega, Madison, WI, USA). For in vivo experiments, tumor tissue homogenate was lysed for western blot analysis [20]. The protein concentration of the lysate was determined by a BCA Protein Assay Kit (Beyotime Biotechnology Co., China). Equal quantities of protein (30-50 μg) were separated by sodium dodecyl sulfate-polyacrylamide gel electrophoresis, transferred to polyvinylidene difluoride membranes (Millipore, Billerica, MA, USA), and blocked with 5% non-fat milk for 80 min at room temperature. The membranes were incubated with specific primary antibodies overnight at 4 °C and probed with corresponding secondary antibodies subsequently for 60 min at room temperature. Then specific protein bands were detected with ECL Select Western Blotting detection reagent (Millipore, Billerica, MA, USA) by chemiluminescence (Tanon 5500, Shang Hai, China). Equal protein loading was normalized by probing with anti-GAPDH antibody. Antibodies to cyclin D3, cyclin E1, CDK2, CDK4, CDK6, p21, Bax, Bcl-2, caspase-3, caspase-9, p53, P-p53, and GAPDH were purchased from Cell Signaling Technology (Danvers, MA, USA).

Animal and tumor xenograft studies

BALB/*c* nude mice (weighing 18–20 g) were used to establish a xenograft model. Mice were administrated a

SMMC7721 cell suspension (5×10^6 cells per 100 µL) by subcutaneous injection. When tumor diameter reached 3 mm, mice were randomly allocated to two groups ($n = 5$ per group). Animals in the treated group were administrated bafilomycin C1 (0.2 mg/kg body weight, dissolved in 60% 1,2-propanediol) once every other day by intraperitoneal injection, and control group were treated with vehicle in the same way. Body weight and tumor size (tumor volume = length (mm) × width (mm) × depth (mm) × π/6) were measured every 4 days. After 20 days of treatment, whole blood of each mouse was collected from the ocular orbit for serum analysis. Then the mice were sacrificed and the tumor was excised. The wet weight of internal organs and tumor of each mouse were recorded. A part of the tumor was prepared for western blot and the other part for paraffin block. The study was performed in strict accordance with the Guide for the Care and Use of Laboratory Animals (Ministry of Science and Technology of China, 2006), and all experimental protocols were approved by the Laboratory Ethics Committees of College of Life and Health Sciences, Northeastern University (Shenyang, China).

Serum analysis

Serum aspartate aminotransferase (AST) and L-alanine 2-oxoglutarate aminotansferase (ALT) changing levels were monitored to evaluate the poisonous side effect of bafilomycin C1 on mice by using the Aspartate Aminotansferase Assay Kit and Alanine Aminotransgerase Assay Kit (Jiancheng Bioengineering Ins., Nanjing, China), respectively, according to the manufacturer's instructions. The enzyme activity was detected by measuring the optical density (510 nm).

Hematoxylin and eosin (H&E) staining

Tumor tissues were fixed in 4% paraformaldehyde, paraffin-embedded, and sectioned at 5 µm. Afterwards, the tissue section was deparaffinized in xylene and rehydrated in a series of graded alcohols. Then the tissue section was stained with H&E (Beyotime Biotechnology Co., Shanghai, China) to visualize histology [21].

Detection of apoptotic cells in situ

Tdt-mediated dUTP nick-end labeling (TUNEL) was performed with an apoptosis detection kit (Millipore, Billerica, MA, USA) to identify the number of apoptosis cells according to the manufacturer's instructions [20].

Statistical analysis

All results were presented graphically as the group mean ± standard deviation (SD) from at least three independent experiments. Student's *t*-test was used to determine differences between two groups using SPSS 13.0 (SPSS Inc., Chicago, IL, USA). The threshold value for acceptance of differences was 5% ($p \le 0.05$) .

Results

Bafilomycin C1 retarded the growth and proliferation of SMMC7721 and HepG2 cells

The effect of bafilomycin C1 (Fig. 1a) on the growth of SMMC7721 and HepG2 cells was assessed by MTT assay. The results showed that bafilomycin C1 retarded the growth and proliferation of SMMC7721 and HepG2 cells in a time- and dose-dependent manner (Fig. 1b). Compared with the control, the viability of SMMC7721 and HepG2 cells was not significantly influenced by the dosage of 0.33–3.3 µM and 1.1–10.0 µM at 24 h, respectively. Hence, the effect of bafilomycin C1 on cell-cycle arrest and apoptosis in vitro was investigated after 24 h of drug exposure to avoid the interference from cell death effect.

Bafilomycin C1 induced G0/G1 phase cell-cycle arrest in SMMC7721 and HepG2 cells

In order to explore the effect of bafilomycin C1 on the cell-cycle progression of SMMC7721 and HepG2 cells, the flow cytometric analysis based on PI staining was used to analyze cell-cycle distribution. As shown in Figure 1c, a typical G0/G1 cell-cycle arrest pattern was observed in SMMC7721 and HepG2 cells after 24 h treatment with bafilomycin C1, although the arrest was partial in SMMC7721 cells at that time point.

In order to explore the underlying mechanism, we examined the mRNA level by real-time qPCR for the expression of several cell-cycle regulatory factors in SMMC7721 cells. As shown in Figure 1d, *cyclin D3*, *cyclin E1*, *CDK2*, *CDK4*, and *CDK6* expression were down-regulated and *p21* expression upregulated significantly after 24 h treatment with bafilomycin C1. Furthermore, western blot analysis demonstrated that bafilomycin C1 also decreased the protein expression of cyclin D3, cyclin E1, CDK2, CDK4, and CDK6 and increased p21 in a dose-dependent manner after treatment with bafilomycin C1 (Fig. 1e, f).

Bafilomycin C1 induced SMMC7721 and HepG2 cells apoptosis

Numerous antitumor agents are known to eliminate tumor cells through apoptotic process [22]. To examine whether bafilomycin C1 induced apoptosis in SMMC7721 cells,

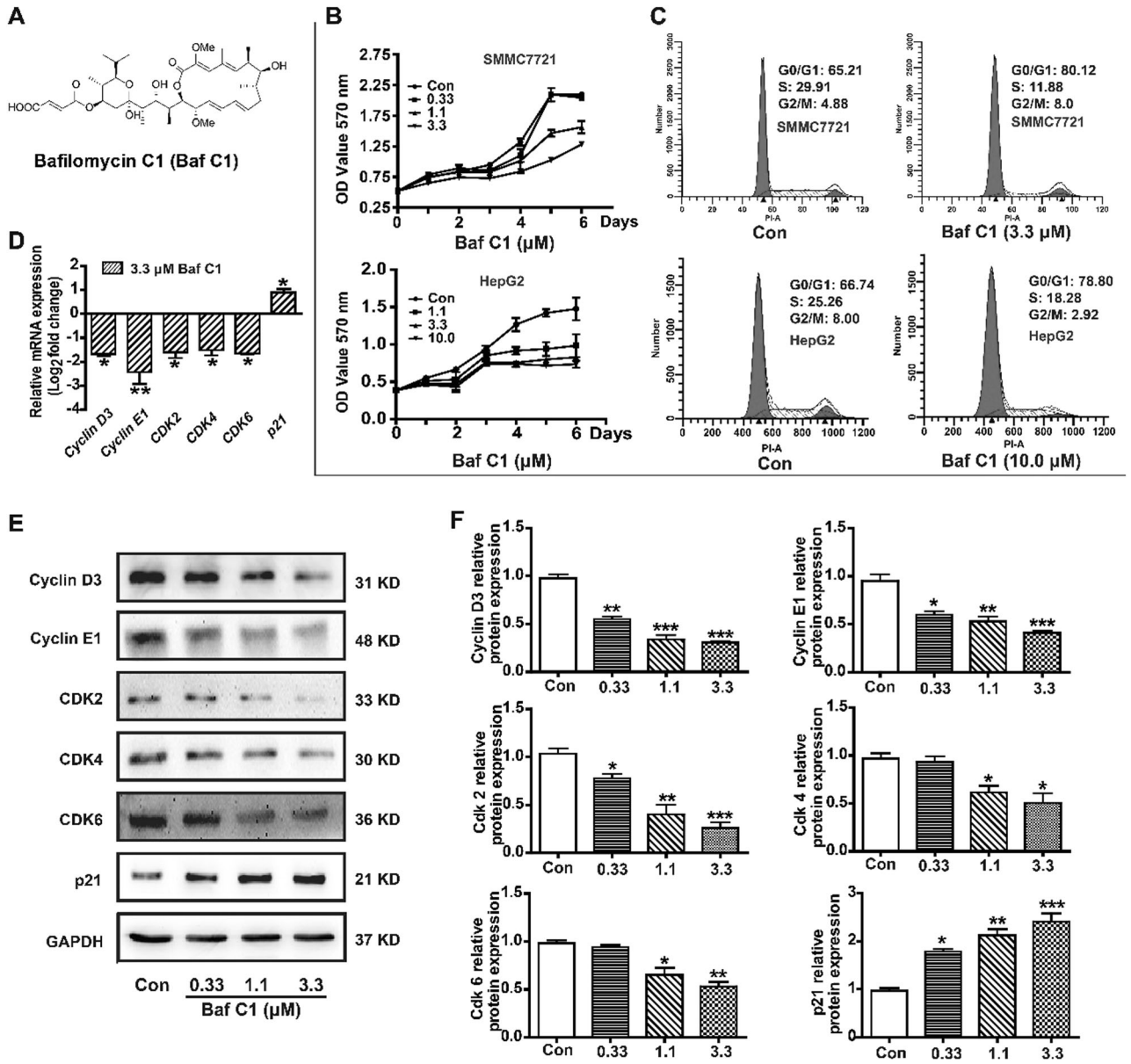

Fig. 1 Bafilomycin C1 retarded the growth and caused cell-cycle arrest in SMMC7721 and HepG2 cells. **a** Chemical structure of bafilomycin C1. **b** The growth curve of SMMC7721 and HepG2 cells treated with vehicle (Con) or different concentrations of bafilomycin C1 (0.33, 1.1, and 3.3 μM for SMMC7721; 1.1, 3.3 and 10.0 μM for HepG2) for 6 days as determined by MTT assay. **c** SMMC7721 and HepG2 cells treated with vehicle (Con) or bafilomycin C1 (3.3 μM for SMMC7721; 10 μM for HepG2) were stained with PI and analyzed for cell-cycle phase by flow cytometry. **d** The mRNA levels of *cyclin D3*, *cyclin E1*, *CDK2*, *CDK4*, *CDK6*, and *p21* of SMMC7721 cells treated with vehicle (Con) or bafilomycin C1 (3.3 μM) were quantified by real-time qPCR. **e** The protein levels of cyclin D3, cyclin E1, CDK2, CDK4, CDK6, and p21 of SMMC7721 cells treated with vehicle (Con) or different concentrations of bafilomycin C1 (0.33, 1.1, and 3.3 μM) were determined by western blot. **f** The relative quantitative analysis of cyclin D3, cyclin E1, CDK2, CDK4, CDK6, and p21 of SMMC7721 cells treated vehicle (Con) or with different concentration of bafilomycin C1 (0.33, 1.1, and 3.3 μM). The results are represented as mean ± SD from three independent experiments. $*p < 0.05$ vs. control; $**p < 0.01$ vs. control; $***p < 0.001$ vs. control

Hoechst 33258 staining was conducted. The results showed that significant morphological changes including nuclei shrinkage, chromatin compaction and dense fluorescence emission were observed in bafilomycin C1-treated SMMC7721 cells (Fig. 2a). Meanwhile, a significant increase in the population of apoptotic cells was identified in bafilomycin C1-treated SMMC7721 cells by flow cytometric analysis based on FITC-Annexin V/PI double staining (Fig. 2b). Similar event also occurred in HepG2 cells, although it was not as strong as that in SMMC7721 cells (Fig. 2b).

Mitochondria play a vital role in supplying energy and are closely involved in apoptosis and cell death [23]. To determine whether bafilomycin C1 affected the function of

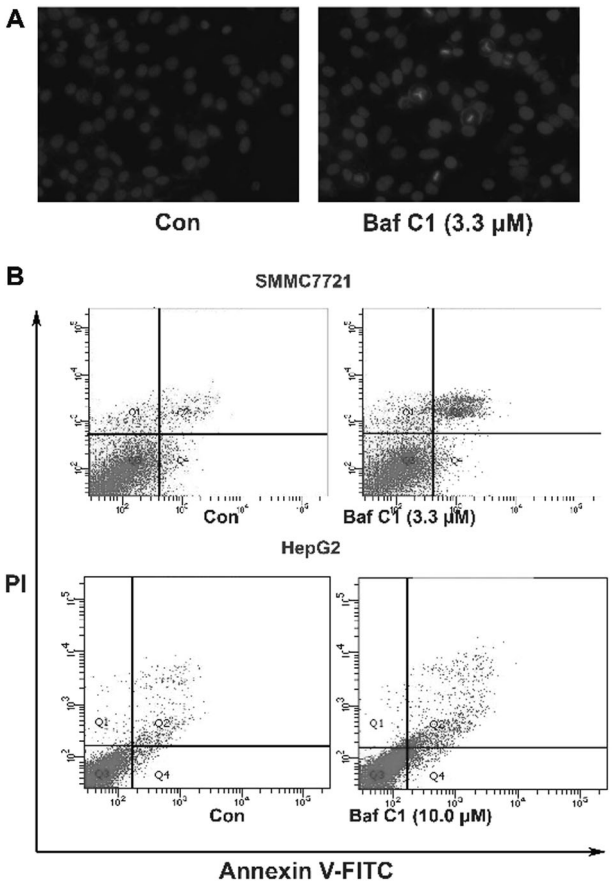

Fig. 2 Bafilomycin C1 induced apoptosis in SMMC7721 and HepG2 cells. **a** Bafilomycin C1 (3.3 μM) caused morphological alterations in SMMC7721 cells as determined by Hoechst 33258 staining compared to vehicle (Con). **b** Bafilomycin C1-induced apoptosis in SMMC7721 and HepG2 cells evaluated by flow cytometric analysis based on FITC-Annexin V and PI double staining compared to vehicle (Con)

mitochondria, we investigated the intracellular ROS production, level of MMP, and ATP generation of SMMC7721 cells treated with bafilomycin C1. As shown in Figure 3a, the level of ROS generation induced by bafilomycin C1 increased significantly in a dose-dependent manner, which was in turn attenuated by the addition of NAC. Furthermore, enhanced MMP collapse and loss of ATP synthesis were also observed after bafilomycin C1 treatment (Fig. 3b, c). As a result, bafilomycin C1 caused mitochondria membrane damage in SMMC7721 cells.

To further examine the underling mechanism, mRNA level of apoptotic-related molecules in SMMC7721 cells was measured. As shown in Figure 3d, the mRNA levels of *Bax* and *p53* increased significantly, whereas the level of *Bcl-2* decreased. Furthermore, western blot was conducted to analyze the change of apoptotic-related proteins. As shown, the protein expression levels of p53, phosphorylated p53 (P-p53), and Bax increased, whereas the level of Bcl-2 decreased significantly in a dose-dependent manner after treatment with bafilomycin C1 (Fig. 3e, f). In addition, the cleavage of caspase-9 and caspase-3 were activated, suggesting that caspase-dependent apoptosis was induced by bafilomycin C1 in SMMC7721 cells (Fig. 3e, f). As a result, bafilomycin C1 induced the mitochondrial apoptotic pathway in SMMC7721 cells.

Bafilomycin C1 retarded xenograft tumor growth in vivo

To evaluate the effect of bafilomycin C1 on tumor growth in vivo, a SMMC7721 cell xenograft model in BALB/*c* nude mice was established. Tumor growth in the bafilomycin C1-treated group was significantly reduced compared to vehicle (Fig. 4a–c). In addition, H&E staining showed the differences of histological features of tumor tissues between the vehicle and bafilomycin C1-treated group. In vehicle, tumor cells exhibited active mitotic increase with big deep-dyed nuclei; however, tumor tissue treated with bafilomycin C1 appeared to have pyknotic nuclei and more necrotic cells (Fig. 4d). Furthermore, we conducted western blot analysis to investigate the mechanism of antitumor effect of bafilomycin C1 in vivo. As shown, the protein expression levels of cyclin D3 and cyclin E1 were downregulated; p21 and cleaved caspase-3 were upregulated in the bafilomycin C1-treated group (Fig. 4e). It suggested that cell-cycle arrest and apoptosis were also induced by bafilomycin C1 in vivo. Moreover, TUNEL assay indicated that bafilomycin C1-treated group appeared to accumulate an increasing number of TUNEL-positive cells, suggesting that more DNA fragmentation, the hallmark of apoptosis, was caused by bafilomycin C1 (Fig. 4f). In addition, physiological and biochemical studies indicated no significant alternations in body weight, liver index, and spleen index as well as serum activities of AST and ALT between the vehicle and treatment group, suggesting that bafilomycin C1 did not result in an increase in severe side effects in the treated mice (Table 1). As a result, bafilomycin C1 suppressed tumor growth through cell-cycle arrest and apoptosis in vivo.

Discussion

Unchecked mitogenic signals and inappropriate response to antimitotic signals caused uncontrolled growth and proliferation of cancer cells [24]. Accumulating evidence confirmed that control of cell-cycle progression in cancer cells was ineffective in controlling tumor growth [24–27]. In our study, bafilomycin C1 significantly induced a partial G0/G1 phase cell-cycle arrest in SMMC7721 cells together with the data obtained from flow cytometry, real-time qPCR, and western blotting analysis. Cell cycle was modulated by different cyclins, cyclin-dependent kinases

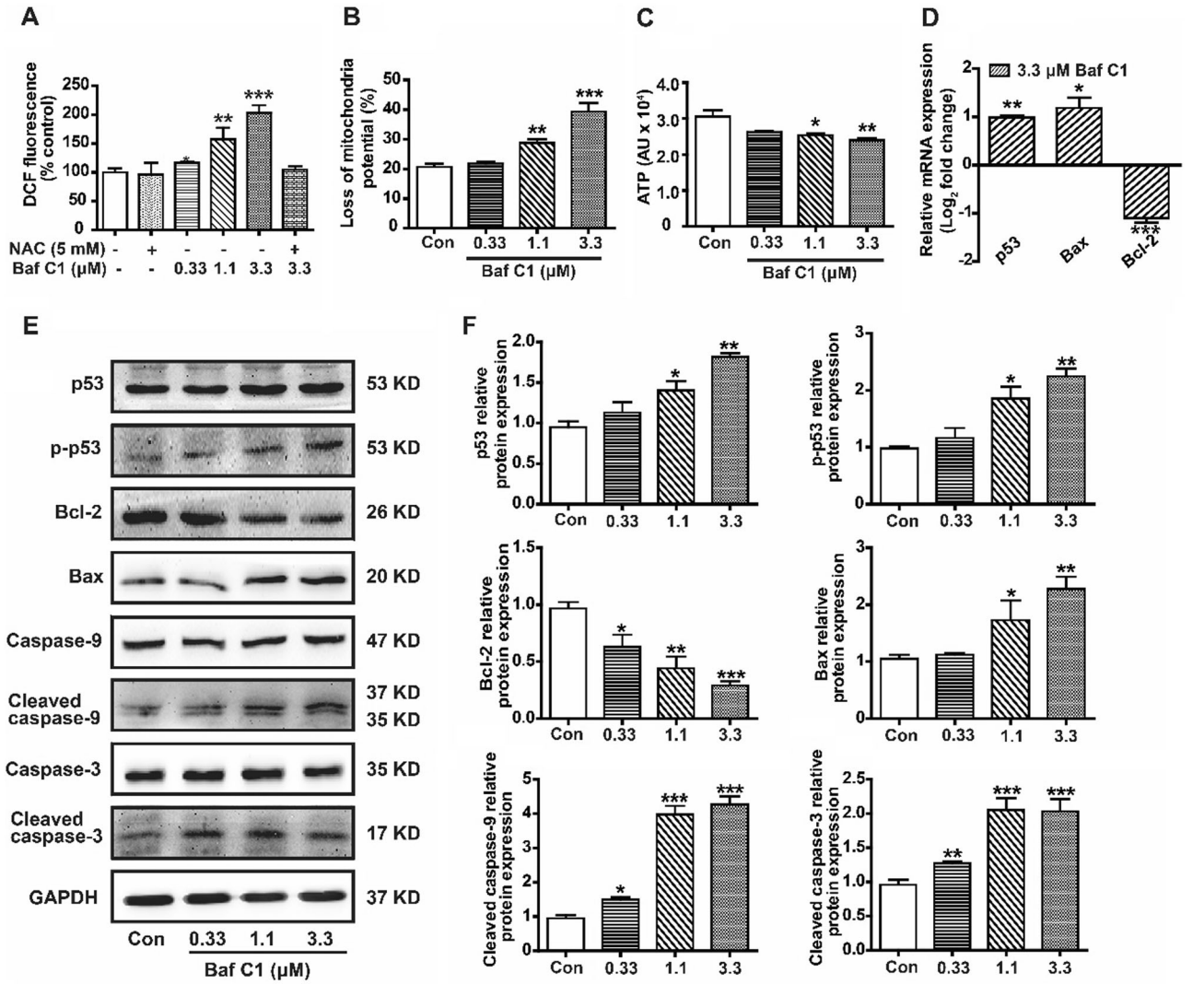

Fig. 3 Bafilomycin C1 caused mitochondrial membrane damage and regulated apoptosis-related molecules of SMMC7721 cells. **a** The intracellular ROS production of SMMC7721 cells treated with vehicle (Con) or different concentrations of bafilomycin C1 (0.33, 1.1, and 3.3 μM) was detected by DCF-DA staining. **b** MMP of SMMC7721 cells treated with vehicle (Con) or different concentrations of bafilomycin C1 (0.33, 1.1, and 3.3 μM) was detected by JC-1 probe. **c** Synthesis of ATP by SMMC7721 cells treated with vehicle (Con) or different concentrations of bafilomycin C1 (0.33, 1.1, and 3.3 μM) was measured by chemiluminescence. **d** The mRNA levels of *p53*, *Bcl-2*, and *Bax* in SMMC7721 cells treated with bafilomycin C1 (3.3 μM) were quantified by real-time qPCR compared to vehicle (Con). **e** The protein levels of p53, P-p53, Bcl-2, Bax, caspase-3, cleaved caspase-3, caspase-9, and cleaved caspase-9 of SMMC7721 cells treated with vehicle (Con) or different concentrations of bafilomycin C1 (0.33, 1.1, and 3.3 μM) were determined by western blot. **f** The relative quantitative analysis of p53, P-p53, Bcl-2, Bax, cleaved caspase-3, and cleaved caspase-9 of SMMC7721 cells treated with vehicle (Con) or different concentrations of bafilomycin C1 (0.33, 1.1, and 3.3 μM). The results are represented as mean ± SD from three independent experiments. $*p < 0.05$ vs. control; $**p < 0.01$ vs. control; $***p < 0.001$ vs. control

(CDKs), and cyclin-dependent kinase inhibitor (CKIs) [24]. Only certain CDK–cyclin complexes were responsible for regulating cell-cycle progression [28]. In G0/G1 phase, cyclin D and cyclin E played vital roles. Cyclin D bound to CDK4 and CDK6 to regulate the early G1 phase, and cyclin E–CDK2 complex peaked at G1/S transition to drive cell cycle progressing to S phase [24, 29, 30]. The detailed mechanistic studies showed that bafilomycin C1 decreased both mRNA and protein levels of cyclin D3, cyclin E1, CDK2, CDK4, and CDK6 in SMMC7721 cells (Fig. 1d–f). On the other side, CKIs, especially p21 in G0/G1 phase, disrupted the activity of CDK–cyclin complex leading to limited cell proliferation and apoptotic cell death consequently [31]. As shown in Figure 1, bafilomycin C1 increased p21 in SMMC7721 cells.

Apoptosis is involved in cell renewal as well as senescent cell elimination and was mediated by a series of sophisticated energy-dependent molecular events [32]. Abnormalities in cell death may also contribute to the development of cancer [33]. Therefore, chemotherapeutic drugs promoting

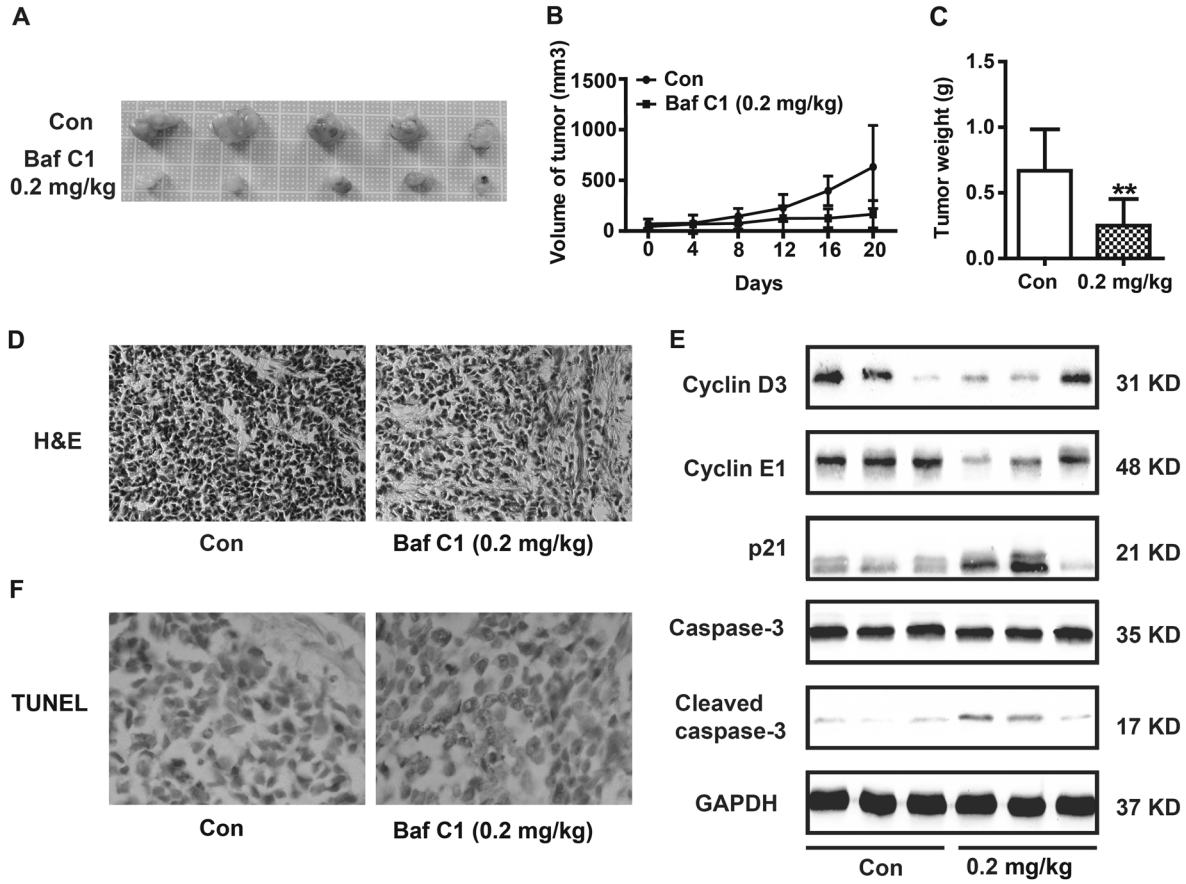

Fig. 4 Bafilomycin C1 suppressed tumor growth of SMMC7721 tumor xenografts in nude mice model. **a** Photographs of individual tumor xenograft removed from nude mice treated with vehicle (Con) or bafilomycin C1 (0.2 mg/kg body weight). **b** The volumes of tumors treated with vehicle (Con) or bafilomycin C1 (0.2 mg/kg body weight) were monitored every 4 days. **c** Tumor weight treated with vehicle (Con) or bafilomycin C1 (0.2 mg/kg body weight) was measured after sacrifice. **d** H&E staining of tumor tissue treated with vehicle (Con) or bafilomycin C1 (0.2 mg/kg body weight). **e** The protein levels of cyclin D3, cyclin E1, p21, caspase-3, and cleaved caspase-3 of tumor tissue treated with vehicle (Con) or bafilomycin C1 (0.2 mg/kg body weight) were determined by western blot. **f** TUNEL assays of tumor tissue treated with vehicle (Con) or bafilomycin C1 (0.2 mg/kg body weight). The results are represented as mean ± SD from five independent experiments. $^{**}p < 0.01$ vs. control

Table 1 Physiological and biochemical index of xenograft nude mice

	Body weight (g)	Liver index (mg/g)	Spleen index (mg/g)	AST (karU)	ALT (karU)
Con	24.2 ± 2.3	54.6 ± 3.9	7.1 ± 1.2	90.4 ± 5.6	75.2 ± 4.0
Bafilomycin C1 (0.2 mg/kg)	22.5 ± 1.6	56.8 ± 1.4	6.95 ± 0.9	94.7 ± 3.1	80.4 ± 4.9

apoptosis may be efficient for the tumor clinical treatment. A series of studies had demonstrated that quite a few chemotherapeutic agent-mediated apoptotic cell death was induced by ROS [34–37]. ROS, which was composed of reactive molecules and free radicals, may lead to oxidative stress of nucleic acid, proteins, and lipids [37–39]. In this study, we found that bafilomycin C1 upregulated the ROS production in SMMC7721 cells (Fig. 3a). The overproduction of ROS triggered the mitochondrial dysfunction, mainly characterized by the loss of MMP [40]. In addition, mitochondria are the site of most ATP generation and mitochondrial dysfunction directly leads to reduced ATP synthesis [37, 38, 41]. As shown, bafilomycin C1 caused the loss of MMP and ATP synthesis (Fig. 3b, c). The Bcl-2 family proteins, which are the key regulators of MMP, exerted opposed effects on apoptosis [41–43]. In our study, bafilomycin C1 upregulated the expression of the proapoptotic factor Bax and downregulated the antiapoptotic Bcl-2 on both mRNA and protein levels (Fig. 3d–f). Enhancement of Bax over Bcl-2 triggered the release of

apoptosis-inducing factors and caused the activation of caspases on the intrinsic apoptotic pathway, which was the hallmark of apoptosis in multiple cell types [44]. Caspase-9, the initiator caspase, was activated by self-proteolysis and triggered the cleavage of caspase-3, the executioner of apoptosis, that finally amplified the apoptotic signaling pathway irreversibly [33, 45, 46]. The present study showed that bafilomycin C1 activated cleaved caspase-9 and cleaved caspase-3 (Fig. 3e, f). Besides, several lines of evidence showed that nuclear transcription factor p53 stimulated a wide network of signals involved in intrinsic or extrinsic apoptotic pathways [47]. The upregulation of total p53 and its phosphorylation (P-p53) validated the effects of bafilomycin C1 on inducing apoptosis.

Furthermore, we investigated the antitumor effects of bafilomycin C1 in SMMC7721 xenograft model. The results showed that bafilomycin C1 retarded the tumor growth without apparent adverse reactions or side effects (Fig. 4a–c; Table 1). H&E staining elucidated the histological changes of tumor tissue treated by bafilomycin C1 (Fig. 4d). In addition, western blot and TUNEL assay showed that the delay in the growth of tumor resulted from cell-cycle arrest and apoptosis caused by bafilomycin C1 (Fig. 4e, f).

In conclusion, bafilomycin C1 effectively induced growth delay, partial cell-cycle arrest, and activated apoptotic pathway of SMMC7721 cells in vitro and in vivo. It indicates that bafilomycin C1 could serve as a potential candidate for hepatic carcinoma chemotherapy.

Acknowledgements This work was funded by National Natural Science Foundation of China (Grant No. 81573327).

Compliance with ethical standards

Conflict of interest The authors declare that they have no conflict of interest.

References

1. Avila MA, Berasain C, Sangro B, Prieto J. New therapies for hepatocellular carcinoma. Oncogene. 2006;25:3866–84.
2. Forner A, Bruix J. Ablation for hepatocellular carcinoma: is there need to have a winning technique. J Hepatol. 2010;52:310–2.
3. Crissien AM, Frenette C. Current management of hepatocellular carcinoma. Gastroenterol Hepatol. 2014;10:153–61.
4. Marquardt JU, Galle PR, Teufel A. Molecular diagnosis and therapy of hepatocellular carcinoma (HCC): an emerging field for advanced technologies. J Hepatol. 2012;56:267–75.
5. Ding N, et al. Bafilomycins and odoriferous sesquiterpenoids from *Streptomyces albolongus* isolated from *Elephas maximus* feces. J Nat Prod. 2016;79:799–805.
6. Werner G, Hagenmaier H, Drautz H, Baumgartner. A, Zähner H. Bafilomycins, a new group of marcrolide antibiotics. J Antibiot. 1984;37:110–7.
7. Moon SS, Hwang WH, Chung YR, Shin J. New cytotoxic bafilomycin C1-amide produced by *Kitasatospora cheerisanensis*. J Antibiot. 2003;56:856–61.
8. Carr G, et al. Bafilomycins produced in culture by *Streptomyces* spp. isolated from marine habitats are potent inhibitors of autophagy. J Nat Prod. 2010;73:422–7.
9. Muench SP, et al. PA1b inhibitor binding to subunits C and E of the vacuolar ATPase reveals its insecticidal mechanism. J Biol Chem. 2014;289:16399–408.
10. Su H, et al. Bafilomycin C1 exert antifungal effect through disturbing sterol biosynthesis in *Candida albicans*. J Antibiot. 2018;71:467–76.
11. Liu Y, Peterson DA, Kimura H, Schubert D. Mechanism of cellular 3-(4,5-dimethylthiazol-2-yl)-2,5-diphenyltetrazolium bromide (MTT) reduction. J Neurochem. 1997;69:581–93.
12. Otsubo T, Akiyama Y, Yanagihara K, Yuasa Y. SOX2 is frequently downregulated in gastric cancers and inhibits cell growth through cell-cycle arrest and apoptosis. Br J Cancer. 2008;98:824–31.
13. Li M, et al. Bigelovin triggered apoptosis in colorectal cancer in vitro and in vivo via upregulating death receptor 5 and reactive oxidative species. Sci Rep. 2017;7:42176.
14. Vermes I, Haanen C, Steffens-Nakken H, Reutelingsperger C. A novel assay for apoptosis. Flow cytometric detection of phosphatidylserine expression on early apoptotic cells using fluorescein labelled Annexin V. J Immunol Methods. 1995;184:39–51.
15. Simon HU, Haj-Yehia A, Levi-Schaffer F. Role of reactive oxygen species (ROS) in apoptosis induction. Apoptosis. 2000;5:415–8.
16. Ma J, et al. 8,9-Epoxyeicosatrienoic acid analog protects pulmonary artery smooth muscle cells from apoptosis via ROCK pathway. Exp Cell Res. 2010;316:2340–53.
17. Li Y, et al. Activation of sirtuin 3 by silybin attenuates mitochondrial dysfunction in cisplatin-induced acute kidney injury. Front Pharmacol. 2017;8:178.
18. Bi X, et al. Anti-inflammatory effects, SAR, and action mechanism of monoterpenoids from *Radix Paeoniae Alba* on LPS-stimulated RAW 264.7 cells. Molecules. 2017;22:e715.
19. Pfaffl MW. A new mathematical model for relative quantification in real-time RT-PCR. Nucleic Acids Res. 2001;29:e45.
20. Jiang X, et al. Diallyl trisulfide inhibits growth of NCI-H460 *in vitro* and *in vivo*, and ameliorates cisplatin-induced oxidative injury in the treatment of lung carcinoma in xenograft mice. Int J Biol Sci. 2017;13:167–78.
21. Guo ZL, et al. The novel thiosemicarbazone, di-2-pyridylketone 4-cyclohexyl-4-methyl-3-thiosemicarbazone (DpC), inhibits neuroblastoma growth *in vitro* and *in vivo* via multiple mechanisms. J Hematol Oncol. 2016;9:98.
22. Häcker G. The morphology of apoptosis. Cell Tissue Res. 2000;301:5–17.
23. Chan DC. Mitochondria: dynamic organelles in disease, aging, and development. Cell. 2006;125:1241–52.
24. Malumbres M, Barbacid M. Cell cycle, CDKs and cancer: a changing paradigm. Nat Rev Cancer. 2009;9:153–66.
25. Graña X, Reddy EP. Cell cycle control in mammalian cells: role of cyclins, cyclin dependent kinases (CDKs), growth suppressor genes and cyclin-dependent kinase inhibitors (CKIs). Oncogene. 1995;11:211–9.
26. Pavletich NP. Mechanisms of cyclin-dependent kinase regulation: structures of Cdks, their cyclin activators, and Cip and INK4 inhibitors. J Mol Biol. 1999;287:821–8.
27. Williams GH, Stoeber K. The cell cycle and cancer. J Pathol. 2012;226:352–64.
28. Malumbres M, Barbacid M. Mammalian cyclin-dependent kinases. Trends Biochem Sci. 2005;30:630–41.

29. Lundberg AS, Weinberg RA. Functional inactivation of the retinoblastoma protein requires sequential modification by at least two distinct cyclin-cdk complexes. Mol Cel Biol. 1998;18:753–61.
30. Harbour JW, Luo RX, Dei Santi A, Postigo AA, Dean DC. Cdk phosphorylation triggers sequential intramolecular interactions that progressively block Rb functions as cells move through G1. Cell. 1999;98:859–69.
31. Sherr CJ, Roberts JM. CDK inhibitors: positive and negative regulators of G1-phase progression. Genes Dev. 1999;13:1501–12.
32. Elmore S. Apoptosis: a review of programmed cell death. Toxicol Pathol. 2007;35:495–516.
33. Weedon D, Searle J, Kerr JF. Apoptosis. Its nature and implications for dermatopathology. Am J Dermatopathol. 1979;1:133–44.
34. Hu C, et al. E Platinum, a newly synthesized platinum compound, induces autophagy via inhibiting phosphorylation of mTOR in gastric carcinoma BGC-823 cells. Toxicol Lett. 2012;210:78–86.
35. He. H, et al. Physalin A induces apoptosis via p53-Noxa-mediated ROS generation, and autophagy plays a protective role against apoptosis through p38-NF-κB survival pathway in A375-S2 cells. J Ethnopharmacol. 2013;148:544–55.
36. Gundala SR, et al. Hydroxychavicol, a betel leaf component, inhibits prostate cancer through ROS-driven DNA damage and apoptosis. Toxicol Appl Pharm. 2014;280:86–96.
37. Yu MO, et al. Reactive oxygen species production has a critical role in hypoxia-induced Stat3 activation and angiogenesis in human glioblastoma. J Neurooncol. 2015;125:55–63.
38. Tang Q, et al. Resveratrol-induced apoptosis is enhanced by inhibition of autophagy in esophageal squamous cell carcinoma. Cancer Lett. 2013;336:325–37.
39. Kiraz Y, Adan A, Kartal Yandim M, Baran Y. Major apoptotic mechanisms and genes involved in apoptosis. Tumor Biol. 2016;37:8471–86.
40. Chen T, Zheng W, Wong YS, Yang F. Mitochondria-mediated apoptosis in human breast carcinoma MCF-7 cells induces by a novel selenadiazole derivative. Biomed Pharmacother. 2008;62:77–84.
41. Wang F, et al. Salinomycin inhibits proliferation and induces apoptosis of human hepatocellular carcinoma cells in vitro and in vivo. PLoS ONE. 2012;7:e50638.
42. Fulda S. Targeting extrinsic apoptosis in cancer: challenges and opportunities. Semin Cell Dev Biol. 2015;39:84–88.
43. Geng YD, et al. Icariside II-induced mitochondrion and lysosome mediated apoptosis is counterbalanced by an autophagic salvage response in hepatoblastoma. Cancer Lett. 2015;366:19–31.
44. Taylor RC, Cullen SP, Martin SJ. Apoptosis: controlled demolition at the cellular level. Nat Rev Mol Cell Biol. 2008;9:231–41.
45. Cohen GM. Caspases: the executioners of apoptosis. Biochem J. 1997;326:1–16.
46. Rai NK, Tripathi K, Sharma D, Shukla VK. Apoptosis: a basic physiologic process in wound healing. Int J Low Extrem Wounds. 2005;4:138–44.
47. Amaral JD, Castro RE, Steer CJ, Rodrigues CM. P53 and the regulation of hepatocyte apoptosis: implication for disease pathogenesis. Trends Mol Med. 2009;15:531–41.